

# Inventory Uncertainty Quantification using TENDL Covariance Data in Fispact-II

J. W. Eastwood,<sup>1</sup> J. G. Morgan,<sup>1</sup> and J-Ch. Sublet<sup>2,\*</sup>

<sup>1</sup>*Culham Electromagnetics Ltd, Culham Science Centre, Abingdon OX14 3DB, United Kingdom*

<sup>2</sup>*United Kingdom Atomic Energy Authority, Culham Science Centre, Abingdon OX14 3DB, United Kingdom*

(Dated: June 17, 2014; Received XX May 2014; revised received XX August 2014; accepted XX September 2014)

The new inventory code FISPACT-II provides predictions of inventory, radiological quantities and their uncertainties using nuclear data covariance information. Central to the method is a novel fast pathways search algorithm using directed graphs. The pathways output provides (1) an aid to identifying important reactions, (2) fast estimates of uncertainties, (3) reduced models that retain important nuclides and reactions for use in the code's Monte-Carlo sensitivity analysis module. Described are the methods that are being implemented for improving uncertainty predictions, quantification and propagation using the covariance data that the recent nuclear data libraries contain. In the TENDL library, above the upper energy of the resolved resonance range, a Monte Carlo method in which the covariance data come from uncertainties of the nuclear model calculations is used. The nuclear data files are read directly by FISPACT-II without any further intermediate processing. Variance and covariance data are processed and used by FISPACT-II to compute uncertainties in collapsed cross-sections, and these are in turn used to predict uncertainties in inventories and all derived radiological data.

## I. INTRODUCTION

FISPACT-II [1] is the new inventory code central to the EASY-II system [2]. This paper focuses on the novel treatment of pathways and uncertainty in the new code. The pathways analysis (Section III) is used to identify the most significant chains of reactions and decays in transmuting the initial inventory to the dominant nuclides at the end of a chosen step. Section IV summarises how estimates of uncertainty are computed using the uncertainties in the cross-sections and decay constants for nuclides on these significant chains. Section V outlines a more complete Monte-Carlo treatment of uncertainties where covariance data are used to find independent input uncertainties and pathways help reduce the problem size. Section VI demonstrates the system capabilities in comparing experimental measurements of decay heat with their associated experimental uncertainty with simulation results also associated with their calculational uncertainty.

## II. FISPACT-II

### A. Capabilities

FISPACT-II is a practical activation-transmutation, source term engineering prediction tool. It automatically

accommodates given nuclear data libraries by using dynamical memory allocation. The four main tasks that it undertakes are

1. extraction, reduction and storage of nuclear and radiological data and covariances from the EAF or ENDF library files (EAF libraries are included because they are still widely used by the fusion community, and they provide valuable cross-validation with earlier work);
2. construction and solution of the rate equations to determine the time evolution of the inventory in response to different irradiation scenarios. These scenarios include
  - (a) a cooling-only calculation;
  - (b) a single irradiation pulse followed by cooling;
  - (c) multiple irradiation pulses where only flux amplitudes change, followed by cooling;
  - (d) multi-step irradiation where flux amplitude, flux spectra and cross-sections may change, followed by cooling.
3. computation and output of derived radiological quantities;
4. subsidiary calculations to identify the key reactions and decays, and to assess the quality of the predictions. The four main subsidiary items are
  - (a) pathways analysis;

---

\* Corresponding author: jean-christophe.sublet@ccfe.ac.uk

- (b) uncertainty calculations from pathways;
- (c) reduced model calculations;
- (d) Monte-Carlo sensitivity and uncertainty calculations.

The current version of the code can undertake pathways and sensitivity calculations for multi-pulse irradiation cases. Self-shielding may be included in the cross-section collapse calculations using either CALENDF [3] probability table data or the universal curve model [4] associated with resonance data (from ENDF6, MF=2 files). The code uses the EAF, TENDL [5] or any ENDF formatted libraries for its nuclear data. With the TENDL libraries, it handles more targets, irradiating projectiles ( $\gamma$ , n, p, d,  $\alpha$ ), provides additional diagnostic outputs (kerma, dpa and gas appm rates) and uses cross-section covariance data from ENDF MF=33 and MF=40 files.

### B. Data Collapse

The TENDL libraries [6] provide cross-sections  $X_i$ ,  $Y_j$  and (by projection using Eqs.(3)-(5)) covariances  $cov(X_i, Y_j)$  in energy bins  $i, j$ . The EAF libraries provide cross-sections and their fractional uncertainties only. Flux ( $\phi_i$ ) weighted collapsed values used by FISPACT-II are given by

$$\bar{X} = \sum_i W_i X_i \quad (1)$$

$$cov(\bar{X}, \bar{Y}) = \sum_{ij} W_i W_j cov(X_i, Y_j) \quad (2)$$

where  $W_i = \phi_i / \sum_j \phi_j$  is a constant for group  $i$  and the sums are over all energy bins. The covariance data in the EAF or TENDL libraries that FISPACT-II recognises are the ENDF-6 [7] NI-type data with LB=1, 5, or 6. Covariance data are stored as fractional values  $F_{kk'}$  in wide energy bins and values are mapped using projection operators  $S_i^k$ , where  $S_i^k = 1$  if energy bin  $i$  overlaps bin  $k$ , and is zero otherwise as illustrated in Fig. 1.

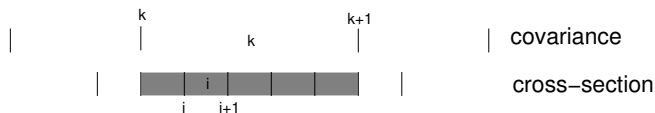


FIG. 1. Projection operator  $S_i^k$  maps cross-section energy bins to covariance energy bins. The shaded energy bins have  $S_i^k = 1$ , and all others have  $S_i^k = 0$ .

Using  $S_i^k$ , the formulae used to construct estimates of the covariance matrix from the library data for LB=1, 5

and 6 are respectively:

$$cov(X_i, X_j) = \sum_{k=1}^K S_i^k S_j^k F_k X_i X_j \quad (3)$$

$$cov(X_i, Y_j) = \sum_{k=1}^K \sum_{k'=1}^K S_i^k S_j^{k'} F_{kk'} X_i Y_j \quad (4)$$

$$cov(X_i, Y_j) = \sum_{k=1}^K \sum_{k'=1}^{K'} S_i^k S_j^{k'} F_{kk'} X_i Y_j \quad (5)$$

where  $K$  and  $K'$  respectively are the number of covariance data energy bins for cross-section data  $X_i$  and  $Y_j$ . FISPACT-II computes collapsed covariances by substituting Equations (3)-(5) in Equation (1) as appropriate. Fission yield data are collapsed in a similar fashion.

## III. PATHWAYS ANALYSIS

### A. Digraph Iteration

The inventory of a given nuclide computed using the rate equations may equivalently be found by a superposition of contributions of flows along a network of pathways to that nuclide, where a pathway is the combination of a linear chain of reactions between different nuclides (a path), plus a number of loops from a nuclide to itself. Pathways analysis finds the significant pathways by automatically combining paths and loops, and these pathways are used in performing uncertainty and sensitivity calculations.

Source nuclides for the pathways calculation are the initial inventory, and target nuclides are dominant nuclides at the current timestep. A dominant nuclide is one that gives a major contribution to a radiological quantity, such as activity, gamma dose, heating, inhalation dosage, etc.

Brute-force searching for pathways rapidly fails owing to the combinatorial growth of possibilities. The novel graph-theoretic algorithm we have developed leads to faster and lower-storage computations. Unimportant branches in the tree are discarded (pruned) to reduce computational complexity. Our algorithm for finding pathways, implemented using linked-list queues, is

1. create a single-visit digraph with edge-weight pruning;
2. iterate on the digraph to extract all edges on significant paths and loops;
3. use these edges to build a tree with weight, loop and depth pruning;
4. combine resulting paths and loops to make pathways;
5. compute inventories along pathways and discard those below a user-specified threshold.

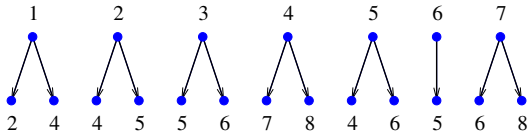


FIG. 2. (Color online) Adjacency list for the 8-nuclide example.

To illustrate the method we consider the eight nuclide example whose adjacency list is shown in Fig. 2. Parent 1 has daughters 2 and 4, etc. To find paths originating at nuclide 1, a single-visit tree is built breadth-first (Fig. 3). At the second level, children of 2 (4 and 5) and 4 (7 and 8) are added. At the third level, children of 4 are not added because nuclide 4 has already been visited as a parent at level 1 and only the first occurrence of nuclide 6 has its children added. The tree is completed at level 4. All the leaves of the tree are nuclides that have appeared earlier.

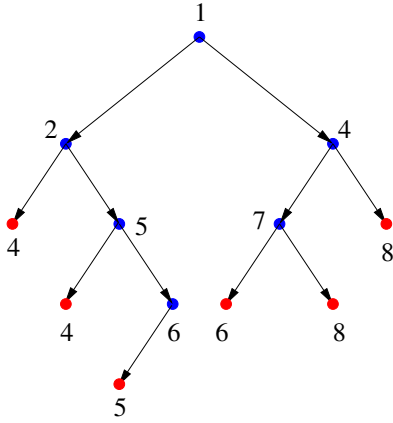


FIG. 3. (Color online) A parent single-visit tree for nuclide 1.

Graph edges are extracted from the digraph of Fig. 3 by iteration. Consider for example paths from nuclide 1 to 4. At the first iteration, edges with nuclide 1 or 4 as children are extracted, giving edges (14), (24) and (54), and adding target nuclides 2 and 5. At the next iteration, edges with children 2 and 5 are extracted, giving edges (12), (25) and (65), and target 6. The third iteration gives (56) and (76) and target 7. The final iteration finds edge (47) and introduces no further target nuclides so the iteration terminates.

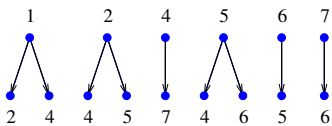


FIG. 4. (Color online) Reduced adjacency list for pathways between nuclides 1 and 4.

Fig. 4 shows the reduced set of edges that are involved in pathways from nuclide 1 to 4. In this trivial example, only nuclide 8 is pruned, but in real cases many are excluded from the reduced adjacency lists. If we excluded pathways with loops on the final nuclide (4), then branches of the full tree could be terminated at occurrences of nuclide 4. Instead, we collect paths and loops separately, and use the following criteria to terminate branches:

1. a loop is found (i.e., a nuclide is encountered that has already occurred on the path from the root to the leaf);
2. the leaf has a weight below the path floor value;
3. the depth exceeds the maximum depth.

In Fig. 5, the solid horizontal (red) line shows a branch terminated by criterion 1, and the broken lines show branches terminated by criterion 2. Traversing the tree reveals paths 1-4, 1-2-4 and 1-2-5-4 at levels 1, 2 and 3, and loop [56] at level 4.

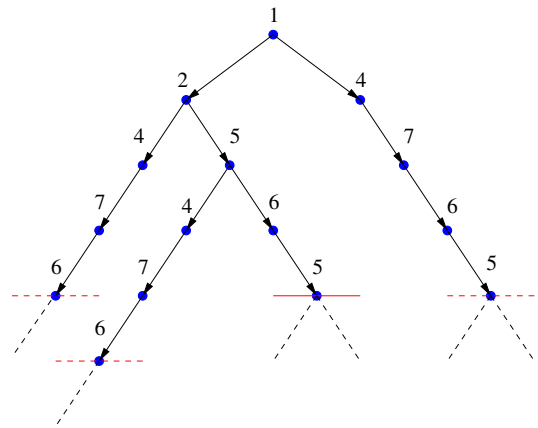


FIG. 5. (Color online) The breadth-first tree for the adjacency list of Fig. 4.

The pruning weight criteria (Section III B below) are sufficient conditions for a pathway to be discarded. The final list is found by integrating the rate equations along the pruned list and discarding those below the chosen thresholds. Fig. 6 shows the resulting pathways from nuclide 1 to 4.

Loops are discarded if they increase the inventory of a path by less than the loop floor fraction. The weights for discarding paths are discussed in the section below.

Note in this example if we had a smaller path floor, then the loop [5476] would have been found and would have been combined with the paths shown in Fig. 6 if its contribution exceeded the loop floor criterion.

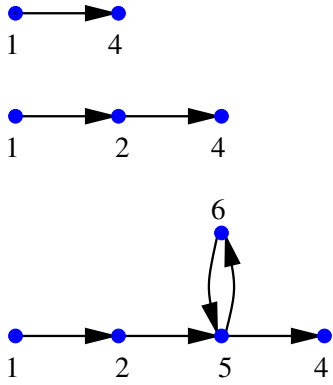


FIG. 6. (Color online) The pathways obtained from the tree in Fig. 5.

### B. Threshold pruning

Pathways are assigned importance based on the fractions of the inventory at the target nuclide that come via them from the source nuclide. Each intermediate step  $i$  from nuclide  $i$  to  $i+1$  along a dominant pathway between the source and the target introduces a reduction in the flow that can be bounded by a reduction factor less than unity.

If  $N_s$  and  $N_t$  are respectively the initial number of source atoms and the final number of target atoms given by the full inventory calculation, and  $\epsilon$  is the threshold fraction of  $N_t$  below which the pathway is not considered significant, then any partial pathway with inventory  $N_D$  at depth  $D$  for which

$$\rho_D = N_D/N_s < \epsilon N_t/N_s \quad (6)$$

can be pruned. Estimated bounds on  $\rho_D$  can be found from the rate equation coefficients and the time interval being considered, but the final pruning and pathway assessment will require integration of the inventory along the pathway.

An upper bound for  $\rho_i$  at level  $i$  can be found by considering the flow along the linear chain that forms a path. The evolution of the inventory is given by

$$\frac{dN_1}{dt} = -\alpha_1 N_1 \quad (7)$$

and for subsequent nuclides ( $i > 1$ )

$$\frac{dN_i}{dt} = -\alpha_i N_i + \beta_{i-1} N_{i-1} \quad (8)$$

where  $\alpha_i$  gives the total rate of decay and induced destruction of a nuclide, and  $\beta_i$  is the rate of decay and transmutation of nuclide  $i$  specifically to nuclide  $i+1$ .

For constant flux,  $\alpha_i$  and  $\beta_i$  are constant, so Equation (8) may be integrated to give

$$N_i(t) = e^{-\alpha_i t} \left( A_i + \int_0^t e^{\alpha_i t'} \beta_{i-1} N_{i-1}(t') dt' \right) \quad (9)$$

where for  $i > 1$ , the initial conditions give  $A_i = 0$ .

The total number of nuclides created at vertex  $i+1$  in time interval  $[0, T]$  is

$$F_{i+1} = \int_0^T \beta_i N_i dt \quad (10)$$

Substituting Equation (9) into Equation (10), interchanging the order of integration and integrating over  $t$  gives

$$\begin{aligned} F_{i+1} &= \frac{\beta_i}{\alpha_i} \left( F_i - e^{-\alpha_i T} \int_0^T dt' N_{i-1}(t') \beta_{i-1} e^{\alpha_i t'} \right) \\ &\leq \frac{\beta_i}{\alpha_i} F_i (1 - e^{-\alpha_i T}) \end{aligned} \quad (11)$$

where the final inequality was obtained by replacing the exponential in the integral by its lower bound ( $= 1$ ) in Equation (11).

Setting  $F_1 = 1$  and computing  $F_{i+1}$  using the inequality in Equation (11) gives an upper bound on  $\rho_i$ , and so provides a sufficient pruning condition for terminating branches in trees such as that illustrated in Fig. 5.

The tree-pruning criterion for a single pulse of irradiation may be extended to multi-pulse irradiation of  $J$  pulses by replacing  $F$  by a vector of length  $J$ . A sufficient condition for the pathway to be discarded at depth  $D$  ( $> 0$ ) is

$$F_{D+1}(T_j) < \epsilon \frac{N_t(T)}{N_s(0)} \quad (12)$$

where this inequality is applied only to the final components of the vectors  $F$  at time  $T_j$ . The total fluxes satisfy initial conditions

$$F_i(T_0) = 0; \quad i > 1 \quad (13)$$

and at the end of time interval  $j$  ( $> 0$ )

$$\begin{aligned} F_{i+1}(T_j) &\leq F_{i+1}(T_{j-1}) \\ &+ \frac{\beta_i^j}{\alpha_i^j} F_i(T_j) [1 - \exp(-\alpha_i^j \Delta T_j)] \end{aligned} \quad (14)$$

where  $\alpha_i^j > 0$ ,  $F_1(T_j) = N_{1,j-1}$  and  $\Delta T_j = T_j - T_{j-1}$ .

Pruning weights using Equations (11)-(14) are implemented in the FISPACT-II pathways calculations.

## IV. UNCERTAINTY ESTIMATES

The pathways, the number of atoms created at target nuclide  $t$  due to the reaction and decay chain along path  $p$  to that nuclide together with uncertainties in the reaction cross-sections and decay half lives associated with the edges of the pathways are used in FISPACT-II to provide estimates of the uncertainties. Pathways arising from a fission are assumed to be correlated and their uncertainties are summed. All other pathway contributions

are treated as uncorrelated and are combined in a random walk approximation. The uncertainty contributions from the reactions along the edges of each pathway are also combined using random walks. If only variances of cross-sections are known, then the cross-sections are assumed to be uncorrelated. If covariance data are known for cross-sections, then the independent variables are obtained by diagonalising the covariance matrix. In deriving the formulae used in FISPACT-II it is also assumed that the number of nuclides formed along path  $p$  of length  $n$  to target nuclide  $t$  at time  $T$

$$N_{tp} = N_{10} \left( \prod_{i=1}^{n-1} \beta_i \right) \sum_{i=1}^n e^{-\alpha_i T} / \prod_{\substack{j=1 \\ j \neq i}}^n (\alpha_i - \alpha_j) \quad (15)$$

may be approximated by

$$N_{tp} = C_{tp} \prod_{i=1}^{n-1} \beta_i \quad (16)$$

where  $C_{tp}$  is a constant along path  $p$  to target  $t$ .

Given a set of target nuclides  $S_t$ , then the uncertainty in some radiological quantity  $Q = \sum_{t \in S_t} q_t$  is given by  $\Delta Q$ , where

$$(\Delta Q)^2 = \sum_{t \in S_t} \left( \frac{\Delta N_t}{N_t} \right)^2 q_t^2 \quad (17)$$

where  $q_t$  may, for example, be activity, gamma dose or some radiotoxicity measure.  $N_t$  is the number of atoms of target nuclide  $t$  formed from the initial inventory and  $\Delta N_t$  is the error in  $N_t$ .  $N_t$  and  $q_t$  are known from the inventory calculation.  $\Delta N_t$  is computed from the pathways inventories and the fractional squared error  $\Delta_{tp}^2$  in the number of atoms of target nuclide  $t$  formed along pathway  $p$  to that target.

If we let the set of pathways to target  $t$  be  $S_p$ , then  $S_p = (\cup_{a \in S_{sa}} S_a) \cup S_o$  where  $S_a$  is the subset of these pathways that start from the fission of an actinide source nuclide  $a$  and  $S_o$  is the set of other pathways.  $S_{sa}$  is the subset of the set of source nuclides that are actinides.

If all the pathways to a target nuclide  $t$  are uncorrelated, then the uncertainty in the inventories along pathways  $p$  to  $t$  can be combined using a random walk approximation to give an estimate of the uncertainty of the target nuclide inventory  $\Delta N_t$ :

$$(\Delta N_t)^2 = \sum_p (\Delta N_{tp})^2 \quad (18)$$

However, pathways arising from a fission are correlated and so are combined linearly:

$$\Delta N_t = \sum_p \Delta N_{tp} \quad (19)$$

Combining these gives the expression for the total  $\Delta N_t$

$$(\Delta N_t)^2 = \sum_{p \in S_o} \Delta N_{tp}^2 + \sum_{a \in S_{sa}} \left( \sum_{p \in S_a} |\Delta N_{tp}| \right)^2 \quad (20)$$

If we treat each cross-section as independent, then on edge  $e$  of a pathway,  $\beta_e = \sigma_e = \sum_r \sigma_r$ , and so from Equation (16), the contribution of reaction  $r$  on edge  $e$  is

$$\delta \left( \frac{\Delta N_{tp}}{N_{tp}} \right) = \frac{\Delta \sigma_r}{\sigma_e} \quad (21)$$

If there are off-diagonal covariance matrix terms for the cross-sections, the independent variables are found by diagonalising the covariance matrix. Let reaction  $r$  belong to the set of reactions  $\{X_1 \dots X_D\}$  for a parent where  $cov(X_i, X_j)$  are nonzero for  $i \neq j$ , then we can find a similarity transformation matrix  $M$  such that  $cov(Y, Y) = M^T cov(X, X) M$  is diagonal with diagonal elements  $var(Y)$ , and  $Y = M^T X$ . Components of  $Y$  are the independent variables, and from Equation (16) the contribution to the uncertainty of inventory  $N_{tp}$  becomes

$$\delta \left( \frac{\Delta N_{tp}}{N_{tp}} \right) = \frac{M_{i(r)j} \Delta Y_j}{\sigma_e} \quad (22)$$

where the dependence of index  $i$  on reaction  $r$  is indicated.

Using the random walk assumption and ignoring any off-diagonal covariance matrix terms gives

$$\begin{aligned} \Delta_{tp}^2 &= \left( \frac{\Delta N_{tp}}{N_{tp}} \right)^2 \\ &= \sum_{e,r} \left( \frac{\Delta \sigma_r}{\sigma_e} \right)^2 + \sum_{e \in D_e} \left( \frac{\Delta \tau_j}{\tau_e} \right)^2 \end{aligned} \quad (23)$$

where the first sum is over all edges  $e$  on each pathway  $p$ , all reactions  $r$  on each edge and over all  $\Delta Y_j = \sqrt{var(Y_j)}$  from the diagonalised covariance matrix for reaction  $r$ . The second term gives the contribution of decay constant uncertainties and is summed over the set of edges. Equation (23) is generalised to handle multi-pulse irradiation scenarios by replacing the first term by

$$\sum_{e,r} \left( \frac{R_r (\Delta \sigma_r / \sigma_r)}{R_e} \right)^2$$

where  $R_r$  and  $R_e$  are respectively the pulse averaged reaction rates of reaction  $r$  and the pulse averaged reaction rate on edge  $e$ .

In FISPACT-II, the pulse averaged fractional squared errors  $\Delta_{tp}^2$  are precomputed from the nuclear data and are used in conjunction with values of  $N_{tp}$  from pathways calculations and  $N_t$  from the main inventory calculation to provide error estimates throughout a calculation.

## V. SENSITIVITY CALCULATION

### A. Monte-Carlo

FISPACT-II uses a Monte-Carlo approach to sensitivity analysis. A series  $S$  of inventory calculations is performed with the set of  $I$  independent variables  $\{X_i^s; i =$

$1, \dots, I; s = 1, \dots, S$  chosen from distributions with means  $\langle X_i \rangle$  and standard deviations  $\langle \Delta X_i \rangle$ . These runs produce a set of  $J$  dependent variables  $\{Q_j^s; j = 1, \dots, J; s = 1, \dots, S\}$ . For the EAF libraries, the cross-sections are treated as the independent variables, but with the TENDL libraries it is possible to take into account covariance data to get a more complete assessment of the uncertainties of results.

The TENDL libraries contain covariance data between some reactions of given parents [6]. FISPACT-II reads these data and collapses the covariances as described in Section II. Given a rank  $D$  symmetric positive definite covariance matrix, we can find a  $D \times D$  similarity transformation matrix  $M$  such that  $Y = M^T X$  and  $cov(Y, Y) = M^T cov(X, X) M$  is diagonal with diagonal elements  $var(Y)$ . The transformed cross-sections  $Y$  are treated as the independent variables, and random samples with means  $\langle Y_i \rangle$  and standard deviations  $\langle \Delta Y_i \rangle$  are chosen, and the input sample cross-sections are computed using  $X = MY$ .

The dependent variables are the numbers of atoms of nuclides  $j$  or some related radiological quantity. The pathways summaries created by pathways analysis provide a good guide as to which cross-sections and decays are likely to be important to include as independent variables in the sensitivity calculation.

Selecting a sensitivity calculation in FISPACT-II causes the series of  $S$  runs with different independent variables to be undertaken to compute, process and output the set  $\{Q_j^s\}$ . The default independent variable distribution is taken to be log-normal, but other options are provided (normal, log-uniform and uniform). Any sequence of irradiation pulses, changes in cross-section, etc. that are possible with FISPACT-II can be used in the sensitivity calculations. The code performs the base calculation with full output, then repeats  $S$  times the sequence of steps with different sets  $\{X_i^s\}$ . The results of the base calculation are not included in the sensitivity calculation.

Sensitivity calculations provide both uncertainty and sensitivity output. Summary uncertainty output of means  $\bar{X}_i$  and  $\bar{Q}_j$  and standard deviations  $\Delta X_i$  and  $\Delta Q_j$  is produced. The code writes tables of means, standard deviations and Pearson correlation coefficients, and outputs the raw data  $\{X_i^s, Q_j^s; i = 1, \dots, I; j = 1, \dots, J; s = 1, \dots, S\}$  to file for possible post-processing.

## B. Model Reduction

FISPACT-II usually runs with the full TENDL-2013 library of 2630 targets and 3873 possible daughter products and decays that are included in the library. Nuclides that are present in the master nuclide index used by the code are included in a calculation. For single inventory calculations, the cpu time used is small (typically less than a minute on a 3GHz desktop PC), with the dominant time often being that taken to read and collapse the 9 Gigabytes of ASCII data in the TENDL-2013 library.

FISPACT-II has the capability to produce a reduced index in a pathways inventory run, where only those nuclides that appear on pathways from the initial inventory to the dominant nuclides are included. Using a reduced index leads to much faster library reading. Memory allocation in the code is all dynamic, and so calculations with a reduced number of nuclides in the index also use less memory.

Sensitivity calculations can also benefit from the model reduction capability. Pathways analysis identifies the important nuclides and reactions. The code has the capability of outputting a reduced master index that includes only those nuclides that appear on the pathways. Repeating calculations using this reduced master index usually accurately reproduces the results from the full calculation. Monte-Carlo sensitivity calculations using the reduced master index will retain the important reactions and decays but will demand smaller cpu time and memory resources. Typical speed-up factors of  $10^4$  without any significant loss of accuracy have been found in some Monte-Carlo validation tests.

## VI. VERIFICATION AND VALIDATION

Careful software lifecycle management under configuration control has been used for the code, unit and integration tests and verification tests. EASY-II is distributed with over 400 input/output regression tests that preserve and extend the verification-validation heritage of EASY-2010 and its predecessors [2].

Figs. 7 and 8 are examples from a validation study against experimental results [8] where experimental results were compared against simulated integral values. The experiment was the JAEA FNS assembly [9] where 14 MeV neutrons were generated by a 2 mA deuteron beam impinging on a stationary tritium bearing titanium target has proven most beneficial.

More than seventy different material samples have been irradiated in sequence to have their decay heat measured in a whole energy absorption spectrometer. The value of those integral results reside mainly in the well characterized and stable neutron spectra at the target position, but also in the time scale of the measurements from a few seconds after irradiation up to 400 days. All experimental results have been compared with values derived from the EASY-II simulation. For both calculated and experimental values uncertainty estimates are also provided.

The FISPACT-II simulations used the random-walk approximation uncertainty estimate methods described in Section IV, where only the covariance data in the TENDL-2013 library between different energy groups  $cov(X_i, X_j)$  of reaction  $X$  were used. All covariance data between different reactions were ignored.

Figs. 7 and 8 demonstrate the validation results for samples of Nickel and Niobium irradiated for 5 minutes at JAEA FNS. Decay heat and its associated uncertainty were measured for both samples at many cooling times ranging from 36s to 1 hour. The short-term decay

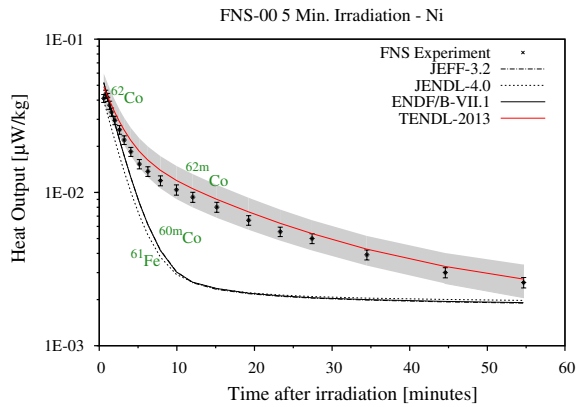


FIG. 7. (Color online) Nickel C/E decay heat comparison, TENDL derived uncertainty as gray area.

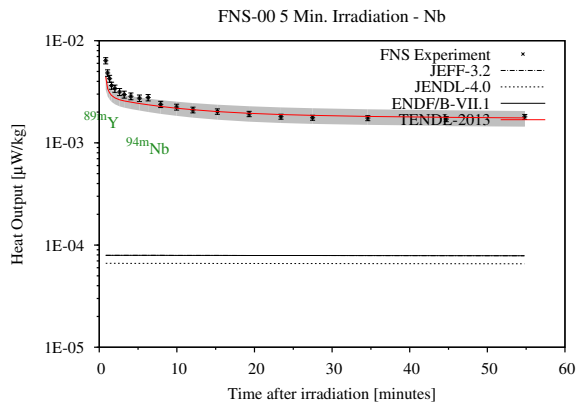


FIG. 8. (Color online) Niobium C/E decay heat comparison, TENDL derived uncertainty as gray area.

heat is well predicted, as the calculational uncertainties (grey areas, circa 24% and 15% respectively) compare with the experimental (vertical bar, circa 8% in both cases) ones when the TENDL-2013 library is used. How-

ever, the code predictions deteriorate when the JEFF-3.2, ENDF/B-VII.1 or JENDL-4.0 libraries are used. All those libraries lack isomeric branching ratio and production pathways;  $^{62m}\text{Co}$  through an  $^{62}\text{Ni}(n,p)$  in Nickel irradiation and  $^{89m}\text{Y}$ ,  $^{94m}\text{Nb}$  through  $^{93}\text{Nb}(n,\alpha)$  and  $(n,\gamma)$  for the Niobium one.

## VII. CONCLUSIONS

FISPACT-II brings new capabilities to the long established family of activation codes. At its core is a rate-equation solver that exploits the nuclear data from the TENDL or any ENDF formatted libraries. It has a powerful pathways analysis capability that can easily identify dominant nuclides and significant reaction and decay pathways, and this is used in the fast uncertainty estimation and the more comprehensive sensitivity analysis and uncertainty calculations using Monte-Carlo methods. The code is also capable of running with reduced models and this can be used to speed up calculations.

This paper has focused on the methods being implemented to use the extended covariance data that are now available with the TENDL libraries, but also less often in other ENDF data libraries. There has been substantial validation work. Further validation work, such as the decay heat validation study [8], is being actively pursued. Both the random-walk (Section IV) and the Monte-Carlo with model reduction (Section V) methods are being evaluated.

Covariance data are used to provide better uncertainty predictions. The use of covariance data between different energy groups of a reaction is already fully implemented and tested. The use of covariance data between different reactions is currently being implemented using the approaches described in this paper.

*Acknowledgements:* This work was funded by the RCUK Energy Programme under grant EP/1501045). To obtain further information on the data and models underlying this paper please contact PublicationsManager@ccfe.ac.uk

- 
- [1] J-Ch. Sublet, J. W. Eastwood and J. G. Morgan, "The FISPACT-II User Manual", Culham Centre for Fusion Energy Report, CCFE-R(11)11 (2013).
- [2] "EASY-II European Activation SYstem", <http://www.ccf.ac.uk/EASY.aspx>.
- [3] J-Ch. Sublet and P. Ribon, "CALENDF-2010: User Manual", Commissariat a l'Energie Atomique report, CEA-R-6277, ISSN 0429-3460, 2011
- [4] E. Martinho *et al.*, "Universal curve of the thermal neutron self-shielding factor in foils, wires, spheres and cylinders", J. RADIOANAL. NUCL. CHEM **261** 637-643 (2004).
- [5] A. Koning *et al.*, "TENDL-2013: TALYS-based Evaluated Nuclear Data Library, <http://www.talys.eu/tendl-2013> (2013)
- [6] A. Koning and D. Rochman, "Modern Nuclear Data Evaluation with the TALYS Code System", NUCL. DATA SHEETS **113**, 2841-2924 (2012).
- [7] Edited by A. Trkov *et al.*, "ENDF-6 Formats Manual", Brookhaven National Laboratory Report, BNL-90365-2009 Rev.2 (2011).
- [8] J-Ch Sublet and M. R. Gilbert, "Decay heat validation, FISPACT-II & TENDL-2013, JEFF-3.2, ENDF/B-VII.1 and JENDL-4.0 nuclear data libraries", Culham Centre for Fusion Energy Report, CCFE-R(14)22 (2014).
- [9] F. Maekawa, *et al.*, "Decay Heat Experiment and Validation of calculation code systems for fusion reactor", Japan Atomic Energy Research Institute report, JAERI 99-055, 1999.